Exploiting Sparsity During the Detection of High-order QAM Signals in Large Dimension MIMO Systems

Oleg Tanchuk and Bhaskar Rao, *Fellow, IEEE*

***Abstract*—This paper proposes a detector for large-scale multiple-input multiple-output (MIMO) systems for 16-QAM constellation and channel knowledge at the receiver. The detector is composed of multiple stages. During the first stage, linear MMSE filter is employed and nearest neighbor quantization is performed resulting in a sub-optimal estimate. In the second stage, the residual in the measurement vector is calculated and the subsequent detector works on the error vector which has additional structure. The error vector is often sparse (has few non-zero components) with the all-zero and lowest energy errors having the largest priors. Large number of antennas reduces the dependencies between error and noise vectors and allows the residual detection problem to be modeled as a linear inverse problem with sparse regularizer. The familiar sparse structure motivates the application of Sparse Bayesian Learning method in the detection. The resulting detector shows promise: the SNR gain over MMSE receiver is ~ 10 dB at a bit error rate (BER) of 10^{-3} for 16-QAM 16×16 system.**

***Index Terms*—MIMO detection, sparsity, sparse bayesian learning, MMSE residual**

I. Introduction

Multiple-input multiple-output (MIMO) antenna systems have attractive diversity and capacity gains [1]. In the near future, large MIMO systems with tens and even hundreds of antennas will be promising due to high spectral efficiency. Massive MIMO is reflective of a base station with large number of antennas communicating with many single-antenna mobile terminals. Let N_t and N_r be the number of transmit and receive antennas respectively. The complex baseband received vector for this MIMO system in ideal flat fading, rich scattering environment can be represented as

$$\mathbf{y} = \mathbf{H}_c \mathbf{x}_c + \mathbf{n}_c \tag{1}$$

Where $\mathbf{x}_c \in Q^{N_t}$ is the transmit vector with Q being the M-QAM modulation alphabet. The received vector is given by $\mathbf{y}_c \in \mathbb{C}^{N_r}$. $\mathbf{H}_c$ is the $N_r \times N_t$ channel gain matrix that is perfectly known at the receiver. Its elements are i.i.d. with distribution $\mathbb{C}\mathcal{N}(0, 2)$. The entries of noise vector $\mathbf{n}_c$ are also i.i.d. with distribution $\mathbb{C}\mathcal{N}(0, 2\sigma_n^2)$. For clarity, the problem will be transformed into real domain

$$\begin{bmatrix} \Re(\mathbf{y}_c) \\ \Im(\mathbf{y}_c) \end{bmatrix} = \begin{bmatrix} \Re(\mathbf{H_c}) & -\Im(\mathbf{H_c}) \\ \Im(\mathbf{H_c}) & \Re(\mathbf{H_c}) \end{bmatrix} \begin{bmatrix} \Re(\mathbf{x}_c) \\ \Im(\mathbf{x}_c) \end{bmatrix} + \begin{bmatrix} \Re(\mathbf{n}_c) \\ \Im(\mathbf{n}_c) \end{bmatrix} \tag{2}$$

This research is supported by the National Science Foundation under Grant No. CCF-1115645 and the Ericsson Endowed Chair funds.

Oleg Tanchuk and Bhaskar Rao are with the Department of Electrical and Computer Engineering, University of California, San Diego.

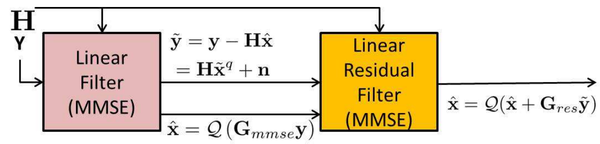

Fig. 1: MMSE-LRR Sequential detector.

$$\mathbf{y} = \mathbf{H}\mathbf{x} + \mathbf{n} \tag{3}$$

Let $N = 2N_t = 2N_r$. Then, $\mathbf{x} \in P^N$ is the transmit vector where P is $\sqrt{M}$-PAM modulation alphabet. $\mathbf{H}$ is now $N \times N$ whose entries come from $\mathcal{N}(0, 1)$. Elements of $\mathbf{n}$ now come from $\mathcal{N}(0, \sigma_n^2)$. Finally, $\mathbf{y} \in \mathbb{R}^N$.

Since noise is Gaussian and transmit priors are uniform, MIMO detection problem can be formulated as minimization of the following l_2 norm

$$\hat{\mathbf{x}}_{\text{ML}} = arg \min_{\mathbf{x} \in P^N} \|\mathbf{y} - \mathbf{H}\mathbf{x}\|^2 \tag{4}$$

One of the key challenges in large MIMO systems is the solution of (4). Global ML-detection is NP-hard problem [2] and is not feasible for large number of antennas. Sphere decoding detectors offer reduction in complexity [3] , but are still very expensive [4]. Several reduced complexity iterative MIMO detectors have been proposed in the past that achieve mixed results for various conditions ([5]–[10]).

Recently, a novel low-complexity LRR (Linear Regression of MMSE Residual) receiver has been proposed [11]. This LRR method consists of two stages as shown in Fig. 1 where $\mathcal{Q}(.)$ implies nearest neighbor quantization. During the first stage, a classic linear minimum mean square error (MMSE) filter is applied to the received vector and the result is quantized. During the second stage, another linear MMSE filter is applied to the quantized residual of the first estimate. Then, the output of the LRR filter is added to the original estimate and the result is quantized. The additional LRR stage results in significant performance improvement for a manageable increase in complexity of the receiver [11].

This paper will build upon this idea of sequential residual detection by exploiting the structure of the quantized error vector. It will be shown that the error vector following MMSE filter usually will have only few non-zero components. This sparsity is amplified as the number of antennas increases. If the dependency between the error vector and the thermal noise is relaxed, MAP estimate of quantized error can be posed as a linear inverse problem with sparse constraint. Sparsity in the context of coding theory was developed in [12] and was used

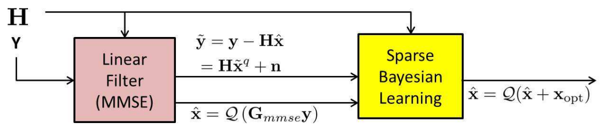

Fig. 2: MMSE-SBL Sequential detector.

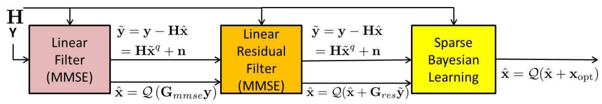

Fig. 3: MMSE-LRR-SBL Sequential detector.

for MIMO detection very recently in [13], but to the best of our knowledge was never applied to MMSE residual.

Various approaches from compressed sensing can be used to solve the resultant MAP equation [14]–[17]. Unfortunately, highly sparse constraints increase the number of local minima [18] which results in convergence errors for these algorithms. Sparse Bayesian Learning (SBL) approach that was first introduced in [19] for classification and applied in [18] to signal processing is well suited for handling local minima at the expense of increased complexity.

In this work we examine two sequential large-scale MIMO receivers. First receiver in Fig. 2 consists of MMSE detector followed by SBL detector of MMSE residual. The second receiver in Fig. 3 consists of MMSE, LRR and SBL detectors. The results are compared to the MMSE-LRR detector from [11] and the classic successive interference canceler first presented in [20] and optimized in [21]. The results show promise for sequential detectors in the context of large MIMO systems.

This paper is organized as follows: section II goes over the MMSE-LRR detector. Section III analyzes the structure of the MMSE residual to set the stage for the application of SBL method in section IV. Simulation results are presented in section V followed by conclusion in section VI.

II. MMSE-LRR Detector

First stage of the low-complexity detector in Fig. 1 is the linear minimum mean square error (MMSE) receiver [22] given by

$$\mathbf{G}_{\text{mmse}} = \arg\min_{\mathbf{G}} \mathbf{E}\left[\|\mathbf{x} - \mathbf{G}\mathbf{y}\|^2\right] \tag{5}$$

The resultant MMSE filter has the following form ([23] [22])

$$\mathbf{G}_{\text{mmse}} = \Sigma_{\mathbf{xy}}\Sigma_{\mathbf{yy}}{}^{-1} = \sqrt{\frac{N}{\sigma_s^2}}\left(\mathbf{H}^T\mathbf{H} + \frac{N}{\rho}\mathbf{I}\right)^{-1}\mathbf{H}^T \tag{6}$$

Where σ_s^2 is the average signal energy and $\rho = \frac{\sigma_s^2}{2\sigma_n^2}$ is the average SNR at the received antenna. The quantized MMSE estimate is given by $\hat{\mathbf{x}} = \mathcal{Q}\left(\mathbf{G}_{\text{mmse}}\mathbf{y}\right)$. MMSE receiver is not optimal and residual can be formed

$$\tilde{\mathbf{y}} = \mathbf{y} - \mathbf{H}\hat{\mathbf{x}} = \mathbf{H}\tilde{\mathbf{x}}^q + \mathbf{n} \text{ where } \tilde{\mathbf{x}}^q = \mathbf{x} - \hat{\mathbf{x}} \tag{7}$$

The LRR filter in [11] then performs another linear MMSE estimate of this residual.

$$\mathbf{G}_{\text{res}} = \Sigma_{\tilde{\mathbf{x}}^q\tilde{\mathbf{y}}}\Sigma_{\tilde{\mathbf{y}}\tilde{\mathbf{y}}}{}^{-1} \tag{8}$$

$$\hat{\mathbf{x}} = \mathcal{Q}(\mathbf{x}_{mmse} + \mathbf{G}_{res}\tilde{\mathbf{y}}) \tag{9}$$

Where local training is used to empirically estimate the correlation matrices $\Sigma_{\tilde{\mathbf{x}}^q\tilde{\mathbf{y}}}$ and $\Sigma_{\tilde{\mathbf{y}}\tilde{\mathbf{y}}}$ [11]. This two-stage solution performs well. For 16×16 16-QAM system, additional detector has gain of 7 dB over MMSE for BER of 10^{-3} [11]. The LRR stage gives a best linear estimate of the error vector ignoring the additional problem structure. Next section explores the properties of the MMSE residual that will be used to improve the subsequent detector.

III. Analysis of MMSE Residual

The quantized error vector $\tilde{\mathbf{x}}^q$ in (7) is discrete and comes from another constellation as shown in Fig. 4. The error constellation represents the differences between all of the original constellation pairs and its cardinality is equal to $(2\sqrt{M} - 1)^2$ for the square M-QAM modulation. Elements of $\tilde{\mathbf{x}}^q$ have few additional properties. Origin is one of the error constellation points and reflects the correct detection by the MMSE receiver. Probability mass function (pmf) of the new constellation will no longer be uniform and will be dependent on the SINR at each stream. The interference term following MMSE must be examined to understand the structure of the pmf. The un-quantized output following MMSE filter is given by

$$\hat{\mathbf{x}} = \mathbf{G}_{\text{mmse}}\mathbf{H}\mathbf{x} + \mathbf{G}_{\text{mmse}}\mathbf{n} = \mathbf{F}\mathbf{x} + \mathbf{G}\mathbf{n} \tag{10}$$

After proper scaling, each stream looks like

$$\hat{\mathbf{x}}_i = \mathbf{x}_i + \frac{1}{\mathbf{F}_{ii}}\sum_{k\neq i}\mathbf{F}_{ik}\mathbf{x}_k + \frac{1}{\mathbf{F}_{ii}}\sum_{k}\mathbf{G}_{ik}\mathbf{n}_k \tag{11}$$

For even moderate N, the co-channel interference term involving $\mathbf{x}_k$ can be approximated by Gaussian distribution. Mean of $\mathbf{x}_k$ and $\mathbf{n}_k$ is zero by definition. Consequently the overall noise term will be zero-mean Gaussian

$$\begin{aligned} \hat{\mathbf{x}}_i &= \mathbf{x}_i + \mathbf{z}_i & \mathbf{z} &= \mathcal{N}\left(0, \Sigma_{\tilde{x}\tilde{x}}\right) \\ \Sigma_{\tilde{\mathbf{x}}\tilde{\mathbf{x}}} &= \left(\tfrac{\rho}{N}\mathbf{H}^T\mathbf{H} + \mathbf{I}\right)^{-1} & \gamma_i &= \frac{1}{(\mathbf{H}^H\mathbf{H}\rho + \mathbf{I})^{-1}_{ii}} - 1 \end{aligned} \tag{12}$$

Where $\Sigma_{\tilde{\mathbf{x}}\tilde{\mathbf{x}}}$ is the MSE matrix and γ_i is the SINR at each stream [22]. The probability of mistaking $\mathbf{x}_k = b$ if $\mathbf{x}_k = a$ was transmitted will be given by the q-function

$$p(b|a) = Q\left(|b - a|\sqrt{\frac{3\gamma_k}{M-1}}\right) \tag{13}$$

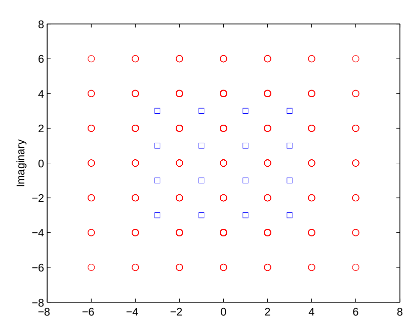

Fig. 4: Original 16-QAM constellation (blue squares) and error constellation (red circles).

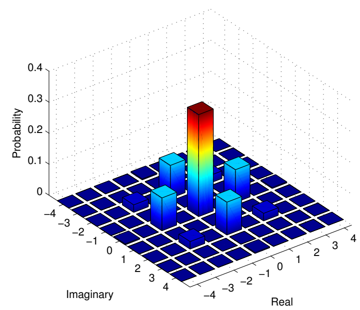

Fig. 5: Quantized error priors of 16-QAM signal following MMSE for SINR of 5 dB.

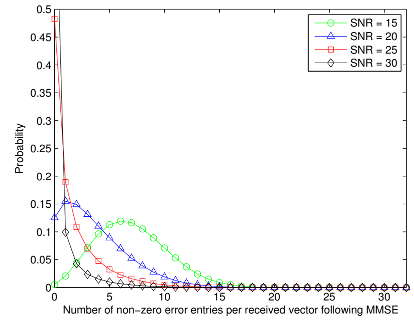

Fig. 7: Probability that quantized error vector following MMSE has a given number of non-zero components for 16-QAM 16×16 system for various SNR.

$$Q(w) = \frac{1}{2\pi} \int_{w}^{\infty} \exp\left(\frac{-w^2}{2}\right) dw \tag{14}$$

Probability of error $\tilde{\mathbf{x}}_k^q = b - a$ will then be a scaled version of (13). Even for moderate γ_k the error prior will drop off quickly with the increase in $|b-a|$. Consequently, we can expect the zero error prior to have largest weight and the bulk of errors to be the nearest neighbor data points. Experimental results confirm this as shown in Fig. 5. In order to apply the Bayesian methods with separable prior and tractable optimization, we need them to be uncorrelated. The error covariance is provided by $\Sigma_{\tilde{\mathbf{x}}\tilde{\mathbf{x}}}$ in (12). Since the elements of the channel matrix are modeled as i.i.d Gaussian, $\mathbf{H}^T\mathbf{H}/N \to I$ as N increases and the diagonal of $\Sigma_{\tilde{\mathbf{x}}\tilde{\mathbf{x}}}$ becomes more dominant as shown in Fig. 6.

With error priors focused on zero and low correlation between $\tilde{\mathbf{x}}_i^q$ we can expect $\tilde{\mathbf{x}}^q$ to be sparse for large N. Fig. 7 shows probability vs. sparsity of $\tilde{\mathbf{x}}^q$ for 16-QAM, 16 x 16 antenna system. It is evident from the plot that with the increase in SNR, the error vector becomes extremely sparse. In the next section we will take advantage of that property in the subsequent detector.

IV. Sparse Bayesian Learning of MMSE Residual

We will examine the detector shown in Fig. 2. Given the residual equation (7) the subsequent detector attempts to maximize the following log-posterior

$$\begin{aligned}\hat{\tilde{\mathbf{x}}}^q &= arg \max_{\tilde{\mathbf{x}}^q} \log P(\tilde{\mathbf{x}}^q|\tilde{\mathbf{y}}) \\ &= arg \max_{\tilde{\mathbf{x}}^q} \log P(\tilde{\mathbf{y}}|\tilde{\mathbf{x}}^q) + \log P(\tilde{\mathbf{x}}^q)\end{aligned} \tag{15}$$

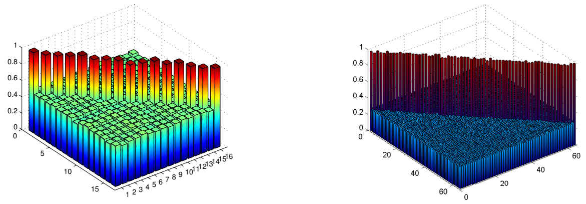

(a) (b)

Fig. 6: Average normalized magnitude of MSE matrix following MMSE for N=16 (a) and N=64 (b).

Where the prior $P(\tilde{\mathbf{x}}^q)$ is sparse and can serve as a regularizer to aid in optimization. This sparse constraint comes at the expense of correlation between the original thermal noise $\mathbf{n}$ and $\tilde{\mathbf{x}}^q$. Additionally, covariance of $\tilde{\mathbf{x}}^q$ is no longer white and $\tilde{\mathbf{x}}^q$ is still discrete. In order to simplify (15) we need to relax these constraints. In section III it was determined that the correlation among the elements of $\tilde{\mathbf{x}}^q$ decreases as N increases. This inclines us to replace the joint pmf of the quantized error vector by a product of one dimensional priors

$$P(\tilde{\mathbf{x}}^q) = \prod_{i=1}^{N_t} P(\tilde{\mathbf{x}}_i^q) \tag{16}$$

Next, we will attempt to replace the sparse discrete pmf by a sparse continuous pdf hoping that the sparsity of the constraint will compensate for the relaxation. Finally, we will ignore the dependency between the noise and the error vector

$$P(\mathbf{n}|\tilde{\mathbf{x}}^q) \sim P(\mathbf{n}) \tag{17}$$

These assumptions result in the following cost function

$$\hat{\tilde{\mathbf{x}}}^q = arg \min_{\tilde{\mathbf{x}}^q} \|\tilde{\mathbf{y}} - \mathbf{H}\tilde{\mathbf{x}}^q\|_2^2 + \lambda \sum_{i=1}^{N_t} g(\tilde{\mathbf{x}}_i^q) \tag{18}$$

Where function $g(\tilde{\mathbf{x}}_i^q)$ reflects the structure of $\log P(\tilde{\mathbf{x}}_i^q)$ and $\lambda = \sigma_n^2$. Optimization problem (18) is a linear inverse problem with sparse constraint that arises in the area of compressed sensing. These types of problems are generally solved in two different ways: MAP estimation (Type I) and Hierarchical Bayesian (Type II) approaches.

Direct minimization of (18) leads to Type I (MAP estimation). Numerous approaches were developed that reflect various degrees of sparsity represented by $g(\tilde{\mathbf{x}}_i^q)$. Example priors are l_1 norm that reflect laplacian prior ([15], [24]), l_p norm with ($p \leq 1$) ([16], [25]) and Jeffrey's prior [17]. These approaches generally can have fast convergence rates with one significant drawback. As the sparsity increases the sparse regularizer becomes concave and overall problem is no-longer convex. For highly sparse constraints such as Jeffrey's prior a lot of local minima emerge. These MAP methods easily get stuck in local minima and result in convergence error. Besides, our model in (15) is a relaxation of the actual posterior and the minimization algorithm should be less sensitive to the additional complexity that was ignored.

Hierarchical Bayesian framework attempts to address these deficiencies by introducing additional latent variables. Many concave functions can be represented as a Gaussian Scale Mixture (GSM) in the following manner [26]

$$P(\tilde{\mathbf{x}}_i^q) = \int P(\tilde{\mathbf{x}}_i^q|\gamma_i)P(\gamma_i)d\gamma_i = \int N(\tilde{\mathbf{x}}_i^q; 0, \gamma_i)P(\gamma_i)d\gamma_i \tag{19}$$

Where $P(\gamma_i)$ dictates the actual shape of $P(\tilde{\mathbf{x}}_i^q)$. Remember that $\tilde{\mathbf{x}}_i^q$ was made continuous. Using this decomposition one can view $\tilde{\mathbf{x}}_i^q$ as nuisance parameters that can be integrated out to find the scale mixture that most closely reflects the residual $\tilde{\mathbf{y}}$ across all possible $\tilde{\mathbf{x}}_i^q$

$$\hat{\gamma} = arg \max_{\gamma} \int P(\tilde{\mathbf{y}}|\tilde{\mathbf{x}}_i^q) \prod_i P(\tilde{\mathbf{x}}_i^q|\gamma_i)P(\gamma_i)d\tilde{\mathbf{x}}^q \tag{20}$$

Integral in (20) can be solved in closed form, resulting the following Type II optimization [19]

$$\hat{\gamma} = arg \min_{\gamma} \log|\mathbf{\Sigma}_{\tilde{\mathbf{y}}}| + \tilde{\mathbf{y}}^T \mathbf{\Sigma}_{\tilde{\mathbf{y}}} \tilde{\mathbf{y}} + \sum_i \log P(\gamma_i) \tag{21}$$

Where $\mathbf{\Sigma}_{\tilde{\mathbf{y}}} = \lambda \mathbf{I} + \mathbf{H}\Gamma\mathbf{H}^T$ and $\mathbf{\Gamma}$ is a diagonal matrix with $\Gamma_{ii} = \gamma_i$. The last term involving the priors of the latent variables is generally ignored [19]. Even without the last term the minimization cannot be performed in closed form and expectation minimization (EM) or fixed point (FP) algorithm is used [19]. EM method requires the knowledge of the posterior of the hidden variables which can be calculated in closed form

$$P(\tilde{\mathbf{x}}^q|\tilde{\mathbf{y}};\gamma) = \frac{P(\tilde{\mathbf{y}}|\tilde{\mathbf{x}}^q) \prod_i P(\tilde{\mathbf{x}}_i^q|\gamma_i)}{\int P(\tilde{\mathbf{y}}|\tilde{\mathbf{x}}^q) \prod_i P(\tilde{\mathbf{x}}_i^q|\gamma_i) d\tilde{\mathbf{x}}^q} = N(\mu_{\mathbf{x}}, \mathbf{\Sigma}_{\mathbf{x}}) \tag{22}$$

Where the posterior mean and covariance are given by

$$\begin{aligned} \mu_{\mathbf{x}} &= \mathbf{\Gamma}\mathbf{H}^T(\lambda I + \mathbf{H}\mathbf{\Gamma}\mathbf{H}^T)^{-1}\tilde{\mathbf{y}} \\ \mathbf{\Sigma}_{\mathbf{x}} &= \mathbf{\Gamma} - \mathbf{\Gamma}\mathbf{H}^T(\lambda\mathbf{I} + \mathbf{H}\mathbf{\Gamma}\mathbf{H}^T)^{-1}\mathbf{H}\mathbf{\Gamma} \end{aligned} \tag{23}$$

The expectation step in the EM algorithm can then be represented as [18]

$$\text{E step: } E_{\tilde{\mathbf{x}}^q|\tilde{\mathbf{y}};\gamma^k}[\log p(\tilde{\mathbf{x}}^q, \tilde{\mathbf{y}}; \gamma)] \rightarrow \text{update } \mathbf{\Sigma}_{\mathbf{x}}\ ,\ \mu_{\mathbf{x}} \tag{24}$$

Followed by maximizaton step

$$\begin{aligned} \text{M step: } \gamma_i^{(k+1)} &= \arg\max_{\gamma_i \geq 0} E_{\tilde{\mathbf{x}}^q|\tilde{\mathbf{y}};\gamma^k}[\log p(\tilde{\mathbf{x}}^q, \tilde{\mathbf{y}}; \gamma)] \\ &= E_{\tilde{\mathbf{x}}^q|\tilde{\mathbf{y}};\gamma^k}[(\tilde{\mathbf{x}}^q)^2] = (\mathbf{\Sigma}_{\mathbf{x}})_{ii} + (\mu_{\mathbf{x}})_i^2 \end{aligned} \tag{25}$$

Then, as a final step nearest neighbor quantization is performed using the posterior mean $\mu_{\mathbf{x}}$ and the original MMSE estimate

$$\hat{\mathbf{x}}_{\text{MMSE-SBL}} = \mathcal{Q}(\mathbf{x}_{mmse} + \mu_{\mathbf{x}}) \tag{26}$$

The SBL algorithm can perform much better than Type I methods because local minima are smoothed away [18]. The increase in performance comes at the expense of complexity. Each EM step contains a matrix multiplication and a matrix inversion. If K is the maximum number of EM iterations, then the upper bound on the overall complexity of SBL step is $O(KN^3)$. By varying K one can trade off performance and complexity.

In the simulations that follow we have also attempted the SBL step following the LRR stage as was shown in Fig. 3

$$\hat{\mathbf{x}}_{\text{MMSE-LRR-SBL}} = \mathcal{Q}(\mathbf{x}_{LRR} + \mu_{\mathbf{x}}) \tag{27}$$

V. Simulation Results

First, four detectors were examined: MMSE, MMSE-LRR [11], MMSE-SBL and SIC [21]. Fig. 8 shows the BER for these detectors for 16-QAM modulation and 16×16 (a) and 64×64 (b) antenna systems respectively. Symbols were gray encoded for each stream. Maximum number of SBL iterations was limited to 50. Local training to generate LRR filter was limited to N^2 as in [11]. For lower dimension (a), MMSE-LRR detector outperforms MMSE-SBL by 2 dB at BER 10^{-3}. Worse performance of MMSE-SBL could be explained by simplification of the MAP equation (15) made in section IV. Correlation between some of the elements of $\tilde{\mathbf{x}}^q$ might still be significant as well as the dependency between the noise $\mathbf{n}$ and $\tilde{\mathbf{x}}^q$. As the number of antennas increases to 64, the average correlation drops and the cost function (18) is closer to the actual posterior. In this case MMSE-SBL outperforms MMSE- LRR by 1 dB at BER 10^{-3}. SIC detector outperforms both MMSE-SBL and MMSE-LRR in either case.

In the second case, we decided to put SBL and LRR stages in sequence and compare its performance to MMSE-LRR and SIC. BER results for the same simulation settings are shown in Fig. 9. SBL stage gives additional 2 dB (a) and 5 dB (b) of performance boost over LRR at BER 10^{-3}. We observe in Fig. 9b that MMSE-LRR-SBL finally outperforms SIC for large number of antennas by 3 dB. Both LRR and SBL detectors perform better with low correlation among the elements of the error vector, but deal with it in different ways. LRR detector spreads the interference across the elements whereas our SBL algorithm ignores it and focuses on the sparsity of the error vector. Different behavior of these two methods allows them to be placed in sequence. SIC detector also benefits from the low correlation among the transmit elements, but this is quickly compensated by a large number of errors when incorrect detection occurs early on and its effect is propagated to subsequent streams. Due to this weakness, SIC cannot take advantage of the increased diversity in the same manner that LRR and SBL can.

The simulations are also being performed for 64-QAM system and will be presented in the follow up work.

VI. Conclusion

We have examined the MMSE error vector and came to a conclusion that it is often sparse. This property was exploited to cast the log posterior of the error vector in the form of linear inverse problem with a sparse constraint. Then, Sparse Bayesian framework was used and EM algorithm utilized to improve the estimate of the transmit vector. SBL detector in sequence with LRR stage shows promising results for large number of antennas and 16-QAM constellations. The subject of the future work will be to get a better representation

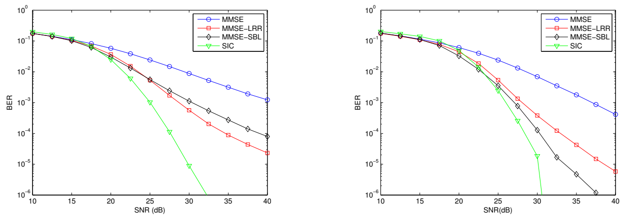

(a) (b)

Fig. 8: BER vs. average received SNR at the antenna for 16-QAM 16×16 (a) and 64×64 (b) systems for MMSE, MMSE-LRR, MMSE-SBL and SIC receivers.

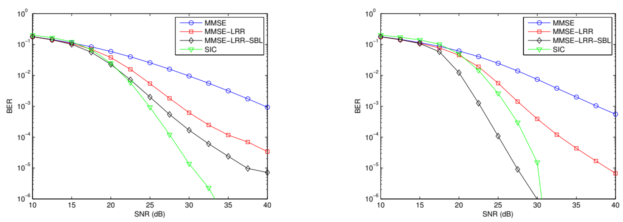

(a) (b)

Fig. 9: BER vs. average received SNR at the antenna for 16-QAM 16×16 (a) and 64×64 (b) systems for MMSE, MMSE-LRR, MMSE-LRR-SBL and SIC receivers.

of (15) by accounting for the dependencies between the variables. Then, EM algorithm will be optimized to reduce the complexity of the SBL stage. The optimal sequence of detectors will also be analyzed.

References

[1] I. E. Telatar, "Capacity of multi-antenna gaussian channels," *Europ. Trans. on Tel.*, vol. 10, pp. 585–595, 1999.

[2] E. Agrell, T. Eriksson, A. Vardy, and K. Zeger, "Closest point search in lattices," *IEEE Trans. on Inf. Th.*, vol. 48, no. 8, pp. 2201–2214, Aug 2002.

[3] U. Fincke and M. Pohst, "Improved methods for calculating vectors of short length in a lattice, including a complexity analysis," *Math. Comput.*, vol. 44, no. 170, pp. 463–471, 1985.

[4] B. Hassibi and H. Vikalo, "On the sphere decoding algorithm i. expected complexity," *IEEE Trans. on Sig. Proc.*, vol. 53, no. 8, pp. 2819–2834, Aug 2005.

[5] K. V. Vardhan, S. K. Mohammed, A. Chockalingam, and B. S. Rajan, "A low-complexity detector for large mimo systems and multicarrier cdma systems," *IEEE JSAC Sp. Issue on Multi. Det. for Adv. Comm. Sys. and Net.*, vol. 28, no. 3, pp. 473–485, April 2008.

[6] Y. Sun, "A family of linear complexity likelihood ascent search detectors for cdma multiuser detection," in *IEEE 6th Intl Symp. on Spread Spec. Tech.*, 2000.

[7] N. Srindhi, T. Datta, A. Chockalingam, and B. S. Rajan, "Layered tabu search algorithm for large-mimo detection and a lower bound on ml performance," *IEEE Trans. on Comm.*, vol. 59, no. 11, pp. 2955–2964, Nov 2011.

[8] P. Som, T. Datta, N. Srinidhi, A. Chockalingam, and B. S. Rajan, "Low-complexity detection in large-dimension mimo-isi channels using graphical models," *IEEE Jl. Sel. Topics in Sig. Proc.*, vol. 5, no. 8, pp. 1497–1511, Dec 2011.

[9] A. Wiesel, Y. Eldar, and S. Shamai, "Semidefinite relaxation for detection of 16-qam signaling in mimo channels," *IEEE Sig. Proc. Lett.*, vol. 12, no. 9, pp. 653–656, 2005.

[10] N. Sidiropoulos and Z. Luo, "A semidefinite relaxation approach to mimo detection for high-order qam constellations," *IEEE Sig. Proc. Lett.*, vol. 13, no. 9, pp. 525–528, 2006.

[11] S. Nagaraja, O. Dabeer, and A. Chockalingam, "Large-mimo receiver based on linear regression of mmse residual," in *Veh. Tech. Conf.* IEEE, 2013, pp. 1–5.

[12] E. J. Candes and T. Tao, "Decoding by linear programming," *IEEE Trans. Inf. Theory*, vol. 51, no. 12, pp. 4203–4215, Dec 2005.

[13] A. Aissa-El-Bey, K. Amis, D. Pastor, and R. Pyndiah, "New iterative detector of mimo transmission using sparse decomposition," *IEEE Trans. on Veh. Tech.*, vol. PP, no. 99, p. 1, 2014.

[14] S. S. Chen, D. L. Donoho, and M. A. Saunders, "Atomic decomposition by basis pursuit," *SIAM J. on Sci. Comput.*, vol. 20, pp. 33–61, 1998.

[15] R. Tibshirani, "Regression shrinkage and selection via the lasso," *J. R. Statist. Soc.*, vol. 58, pp. 267–288, 1994.

[16] I. F. Gorodnitsky and B. D. Rao, "Sparse signal reconstruction from limited data using focuss: a re-weighted minimum norm algorithm," *IEEE Trans. on Sig. Proc.*, vol. 45, no. 3, pp. 600–616, March 1997.

[17] C. Fevotte and S. J. Godsill, "Blind separation of sparse sources using jeffrey's inverse prior and the em algorithm," in *Independent Component Analysis and Blind Signal Separation*. Springer, 2006, pp. 593–600.

[18] D. P. Wipf and B. D. Rao, "Sparse bayesian learning for basis selection," *IEEE Trans. on Sig. Proc.*, vol. 52, no. 8, pp. 2153–2164, Aug. 2004.

[19] M. E. Tipping, "Sparse bayesian learning and the relevance vector machine," *The Journal of Machine Learning Research*, vol. 1, pp. 211–244, Sep 2001.

[20] P.W.Wolniansky, G.J.Foschini, G. Golden, and R. Valenzuela, "V-blast: an architecture for realizing very high data rates over the rich-scattering wireless channel," in *Signal, Systems, and Electronics*. IEEE, 1998, pp. 295–300.

[21] D. Wubben, R. Bohnke, V. Kuhn, and K.-D. Kammeyer, "Mmse extension of v-blast based on sorted qr decomposition," in *Veh. Tech. Conf.*, vol. 1. IEEE, 2003, pp. 508–512.

[22] S. M. Kay, *Fundamentals of Statistical Signal Processing, Volume I: Estimation Theory*. Upper Saddle River, N.J.: Prentice Hall PTR, 1993, vol. 1.

[23] A. Paulraj, R. Nabar, and D. Gore, *Introduction to Space-Time Wireless Communications*. Cambridge Univ. Press New York, NY, USA, 2003.

[24] Y. Lin and D. Lee, "Bayesian l_1-norm sparse learning," in *Int. Conf. on Acoustics, Speech, and Sig. Proc.*, vol. 5. IEEE, May 2006.

[25] B. D. Rao, K. Engan, S. F. Cotter, J. Palmer, and K. Kreutz-Delgado, "Subset selection in noise based on diversity measure minimization," *IEEE Trans. on Sig. Proc.*, vol. 51, no. 3, pp. 760–770, 2003.

[26] J. A. Palmer, D. P. Wipf, K. Kreutz-Delgado, and B. D. Rao, "Variational em algorithm for non-gaussian latent variable models," in *Adv. in Neural. Inf. Proc. Sys.*, 2005, pp. 1059–1066.